

## Complexation of Mercury(I) and Mercury(II) by 18-Crown-6: Hydrothermal Synthesis of the Mercuric Nitrite Complex

Neil J. Williams,<sup>†</sup> Robert D. Hancock,<sup>\*,†</sup> Joseph H. Riebenspies,<sup>‡</sup> Manuel Fernandes,<sup>§</sup> and Alvaro S. de Sousa<sup>\*,§</sup>

<sup>†</sup>Department of Chemistry and Biochemistry, University of North Carolina at Wilmington, Wilmington, North Carolina 28403, <sup>‡</sup>Department of Chemistry, Texas A&M University, College Station, Texas 77843, and <sup>§</sup>School of Chemistry, University of the Witwatersrand, Johannesburg 2050, South Africa

Received September 4, 2009

A dimercury(I) 18-crown-6 complex is isolated, and its possible role in the hydrothermal preparation of the mercuric nitrite complex is discussed. The reported structures are of  $[\text{Hg}_2(18\text{-crown-6})_2(\text{H}_2\text{O})_2](\text{ClO}_4)_2$  (**1**), monoclinic,  $C2/c$ ,  $a = 21.0345(9)$ ,  $b = 12.1565(5)$ ,  $c = 16.8010(7)$  Å,  $\beta = 113.2000(10)^\circ$ ,  $V = 3948.7(3)$  Å<sup>3</sup>,  $Z = 16$ ,  $R = 0.0230$ ;  $[\text{Hg}(18\text{-crown-6})](\text{NO}_2)_2$  (**2**), monoclinic,  $P2_1/c$ ,  $a = 8.027(5)$ ,  $b = 14.437(9)$ ,  $c = 7.827(5)$  Å,  $\beta = 95.165(11)^\circ$ ,  $V = 905.6(10)$  Å<sup>3</sup>,  $Z = 2$ ,  $R = 0.0175$ . The complex cation in compound **1** consists of a mercurous dimer exhibiting a Hg–Hg bond length of 2.524(2) Å. Non-bonding interactions between adjacent crown ether macrocycles across the Hg–Hg bond result in large variations in mercury to oxygen distances within equatorial coordination sites. At low pH compound **1** is proposed to be preferentially formed under hydrothermal conditions affording compound **2** upon disproportionation. Nitrite ions ligate via a unidentate nitrito (*cis to metal*) coordination mode as interpreted using vibrational (infrared) spectroscopy. The conformation adopted by 18-crown-6 in compounds **1** and **2** is closely related to a  $D_{3d}$  conformation as evidenced by X-ray crystallography. Band splitting readily observed in vibrational spectra of the metal free crown ether, attributed to vibrational modes of oxyethylene fragments, is absent in spectra of **1** and **2** confirming a regular  $D_{3d}$  macrocyclic orientation. Short Hg–O bonds observed for axially coordinated water molecules in **1** and coordinated nitrite ligands in **2**, illustrate the prevalence of relativistic effects commonly observed in mercury complexes.

### Introduction

Sensing mercury species in aqueous solution is almost exclusively centered upon recognition of the mercuric ion, interpreted as total analyte concentration. Although the mercurous ion enjoys relative stability in aqueous solution, especially at low pH where metal ion solubility and mobility is enhanced, mercurous complexes and their influence upon the sensing of mercury species is largely unrecognized. The serendipitous formation of a mercurous complex in neutral water, because of unanticipated reduction of a mercuric counterpart, emphasizes the significance of the mercurous ion in the detection of mercury species in aqueous solution.<sup>1</sup> Early literature reports difficulties in determining the composition of dimercury(I) complexes,  $[\text{L}_2\text{Hg}_2]^{2+}$ , as the dimeric mercurous ion,  $\text{Hg}_2^{2+}$ , forms relatively few complexes.<sup>2–4</sup> A logical synthetic approach for  $[\text{L}_2\text{Hg}_2]^{2+}$  complexes involves the addition of a solution of a mercurous salt to a ligand

solution, with appropriate solvent choice affording the complex as a precipitate. Complexes synthesized in this manner are inevitably of low purity, contaminated by analogous complexes of the mercuric ion. More basic ligands show enhanced complex stability for the mercuric ion and promote disproportionation. Complexation studies<sup>5,6</sup> using heterocyclic nitrogen donor ligands indicate disproportionation impedes isolation of the complexed mercurous dimer. Introduction of electron withdrawing substituents<sup>6–8</sup> or steric interactions<sup>5</sup> between metal ion and complexing ligand effectively decreases the basicity of the nitrogen donor atom facilitating the isolation of  $[\text{L}_2\text{Hg}_2]^{2+}$  complexes. Predictably,  $[\text{L}_2\text{Hg}_2]^{2+}$  complexes of oxygen donor ligands are more readily synthesized but are relatively few in number.

Dimercury(I) complexes have, however, been synthesized and isolated from other oxidation states of mercury. Metallocryptands of zerovalent Platinum and Palladium are reported to successfully complex the mercurous dimer.<sup>9</sup>

\*To whom correspondence should be addressed. E-mail: alvaro.desousa@wits.ac.za (A.S.d.S.), hancockr@uncw.edu (R.D.H.).

(1) Ho, M.-L.; Chen, K.-Y.; Wu, L.-C.; Shen, J.-Y.; Lee, G.-H.; Ko, M.-J.; Wang, C.-C.; Lee, J.-F.; Chou, P.-T. *Chem. Commun.* **2008**, 2438–2440.

(2) Sherrill, M. S.; Skowronski, S. *J. Am. Chem. Soc.* **1905**, 27, 30–47.

(3) Faragher, W. F.; Morrell, J. C.; Comay, S. *J. Am. Chem. Soc.* **1929**, 51, 2774–2781.

(4) Morgan, G. T.; Mos, H. W. *J. Chem. Soc.* **1914**, 105, 189.

(5) Taylor, D. *Aust. J. Chem.* **1976**, 29, 723–730.

(6) Kepert, D. L.; Taylor, D. *Aust. J. Chem.* **1974**, 27, 1199–1202.

(7) Kepert, D. L.; Taylor, D.; White, A. H. *Inorg. Chem.* **1972**, 11, 1639–1643.

(8) Kepert, D. L.; Taylor, D.; White, A. H. *J. Chem. Soc., Dalton Trans.* **1973**, 893–896.

(9) Catalano, V. J.; Malwitz, M. A.; Bruce, C. N. *Inorg. Chem.* **2002**, 41, 6553–6559.

**Table 1.** Formation Constants<sup>30</sup> for 18-crown-6; Dicyclohexo-18-crown-6, and 15-crown-5 Complexes of Hg<sub>2</sub><sup>2+</sup> and Hg<sup>2+</sup> at 25°C and  $\mu = 0.1$  M

ligand	log <i>K</i> (Hg <sup>2+</sup> )	log <i>K</i> (LHg <sub>2</sub> <sup>2+</sup> )	log <i>K</i> (L <sub>2</sub> Hg <sub>2</sub> <sup>2+</sup> )
15-crown-5	1.68	a	a
18-crown-6	2.42	a	a
dicyclohexo-18-crown-6			
<i>cis-syn-cis</i>	2.75	1.93	0.6–1.8 <sup>b</sup>
<i>cis-anti-cis</i>	2.60	1.57	1.1

<sup>a</sup> Undetermined. <sup>b</sup> Correlated thermodynamic data prevents accurate determination.

Synthesis of these complexes requires the refluxing of the metallocryptand ligand solution in dichloromethane over elemental mercury under inert conditions. The source of the mercurous dimer is explained using a two-step redox process: an oxidative addition reaction between solvent and the zerovalent platinum or palladium, followed by further reaction with elemental mercury to generate the mercurous ion. Mercuric salts have also been utilized in syntheses of [L<sub>2</sub>Hg<sub>2</sub>]<sup>2+</sup> complexes. In syntheses using mercuric salts the formation of the mercurous ion is attributed to the role of the solvent<sup>10</sup> or ligand<sup>11</sup> as a feasible reducing agent. The solubility of sulfur-containing anthraquinone macrocycles is enhanced in dimethylformamide that is reported to reduce the mercuric ion affording a [L<sub>2</sub>Hg<sub>2</sub>]<sup>2+</sup> complex.<sup>10</sup> NMR studies suggest a tetradentate tripodal nitrogen ligand, tris-[(2-(6-methylpyridyl)methyl)amine], acts as a reducing agent in the synthesis of a [L<sub>2</sub>Hg<sub>2</sub>]<sup>2+</sup> complex using mercuric perchlorate in acetonitrile.<sup>11</sup> Mercury complexes<sup>12–18</sup> of 18-crown-6 reported in the Cambridge Crystallographic Database are inevitably of the higher oxidation state suggesting a preference for complexation of the mercuric ion. Not surprisingly synthesis of the asymmetric [LL'Hg<sub>2</sub>]<sup>2+</sup> complex using 18-crown-6 and 15-crown-5 is performed over elemental mercury, curtailing disproportionation.<sup>19</sup> Equilibrium constant data for the disproportionation of Hg<sub>2</sub><sup>2+</sup> is reported as  $1.14 \times 10^{-2}$ <sup>20</sup> and  $4.3 \times 10^{-3}$ ,<sup>21</sup> corresponding to log *K* values of 1.94 and 2.37, respectively. Ligands capable of stable complexation of the mercuric ion, promoting disproportionation, require a formation constant (log *K*) with the mercuric ion that is substantially larger than 2.37.

Formation constants for mercuric complexes of 18-crown-6 and 15-crown-5 (Table 1) hardly satisfy this prerequisite. Synthesis of [LHg<sub>2</sub>]<sup>2+</sup> and [L<sub>2</sub>Hg<sub>2</sub>]<sup>2+</sup> complexes of these crown ethers may be possible from mercurous salts or through

serendipitous reduction of their mercuric counterparts. Larger formation constants for the mercuric complexes of dicyclohexo-18-crown-6 imply disproportionation of the Hg<sub>2</sub><sup>2+</sup> ion is promoted by this ligand upon complexation. However, formation constants are reported for [LHg<sub>2</sub>]<sup>2+</sup> and [L<sub>2</sub>Hg<sub>2</sub>]<sup>2+</sup> complexes of the *cis-syn-cis* and *cis-anticis* isomers. The Dicyclohexo-18-crown-6 ligand backbone is that of 18-crown-6 with fused cyclohexenyl bridges across donor atoms. Grafting of rigid cyclohexenyl bridges across nitrogen donor atoms in a *trans* arrangement enhances selectivity for metal ions of smaller ionic radius<sup>22–26</sup> but in crown ethers, the *trans* cyclohexenyl bridge across neutral oxygen donors, produces a large decrease in complex stability.<sup>27–29</sup> A *cis* bridging arrangement, for dicyclohexo-18-crown-6, imparts additional stability to the mercuric complexes of the *syn* and *anti* conformational isomers when compared to 18-crown-6<sup>27,30</sup> (Table 1).

Crystallographic data<sup>31</sup> reports the mercuric complex of dicyclohexo-18-crown-6 to be isostructural with Pb<sup>2+</sup> and Sr<sup>2+</sup> analogues. Importantly, lone pair electrons on Pb<sup>2+</sup> are stereochemically inactive when complexed by dicyclohexo-18-crown-6, and ligand conformations in Pb<sup>2+</sup> complexes are representative of ligand conformations in complexes of Hg<sup>2+</sup> and Hg<sub>2</sub><sup>2+</sup>. Conformations, originating from isostructural Pb<sup>2+</sup> complexes, are used to illustrate (Figure 1) relative orientations adopted by dicyclohexo-18-crown-6 when forming a (L<sub>2</sub>Hg<sub>2</sub>)<sup>2+</sup> complex. Steric interactions between adjacent dicyclohexo-18-crown-6 ligands across a Hg–Hg bond, typically observed in [L<sub>2</sub>Hg<sub>2</sub>]<sup>2+</sup> metal clusters including a quasi-linear Hg–Hg–O unit, influence complex stability, and the *cis-syn-cis* complex is entropically favored.<sup>30</sup> Interactions between bulky cyclohexenyl groups cannot be avoided by the *cis-anticis* isomer (Figure 1a, 1b) in which the macrocyclic cavity closely resembles the preferred *D*<sub>3d</sub> conformation associated with 18-crown-6 in mercuric complexes. Face-to-face orientation of *cis-syn-cis* dicyclohexo-18-crown-6 ligands (Figure 1c) minimizes interactions between cycloalkyl groups, and a distorted macrocyclic ring better accommodates relativistic effects, permitting longer Hg–O contacts with macrocyclic oxygen donors, common in mercury complexes. Recent spectroscopic studies on Hg<sup>2+</sup> complexation by a diaza-18-crown-6 derivative proposed the coordination of two Hg<sup>2+</sup> ions confirmed by a structural analysis to be the Hg<sub>2</sub><sup>2+</sup> ion contained within the macrocyclic cavity.<sup>1</sup> In this publication we report the isolation of a symmetric [L<sub>2</sub>Hg<sub>2</sub>]<sup>2+</sup> complex of 18-crown-6 from an Hg<sup>2+</sup> alcohol/water solution in the absence of elemental mercury. The crown ether is an unlikely

- (10) Kadarkaraisamy, M.; Sykes, A. G. *Polyhedron* **2007**, *26*, 1323–1330.  
 (11) Bebout, D. C.; Bush, J. F., II; Shumann, E. M.; Viehweg, J. A. *J. Chem. Cryst.* **2003**, *33*, 457–463.  
 (12) Jaworski, J. S.; Lewicka, A.; Anulewicz, R. *J. Inclusion Phenom. Macrocyclic Chem.* **2003**, *46*, 207–211.  
 (13) Paige, C. R.; Richardson, M. F. *Can. J. Chem.* **1984**, *62*, 332–335.  
 (14) Luis, S. V.; Frias, J. C.; Salvador, R. V.; Bolte, M. *J. Chem. Crystallogr.* **1999**, *29*, 403–408.  
 (15) Pears, D. A.; Stoddart, J. F.; Crosby, J.; Allwood, B. L.; Williams, D. J. *Acta Crystallogr., Sect. C* **1986**, *42*, 51–53.  
 (16) Drew, M. G. B.; Lee, K. C.; Mok, K. F. *Inorg. Chim. Acta* **1989**, *155*, 39–43.  
 (17) Costero, A. M.; Villarroya, J. P.; Gil, S.; Aurell, M. J.; de Arellano, M. C. R. *Tetrahedron* **2002**, *58*, 6729–6734.  
 (18) Rogers, R. D.; Bond, A. H.; Wolf, J. L. *J. Coord. Chem.* **1993**, *29*.  
 (19) Malleier, R.; Kopacka, H.; Schuh, W.; Wurst, K.; Peringer, P. *Chem. Commun.* **2001**, 51–52.  
 (20) Cotton, F. A.; Wilkinson, G.; Murillo, C. A.; Bochmann, M. *Advanced Inorganic Chemistry* 6th ed.; Wiley: New York, 1999.  
 (21) Housecroft, C. E.; Sharpe, A. G. *Inorg. Chem.*, 3rd ed.; Pearson Prentice Hall: New York, **2008**.

- (22) de Sousa, A. S.; Croft, G. J. B.; Wagner, C. A.; Michael, J. P.; Hancock, R. D. *Inorg. Chem.* **1991**, *30*, 3525.  
 (23) de Sousa, A. S.; Hancock, R. D. *J. Chem. Soc., Dalton Trans.* **1997**, 939.  
 (24) de Sousa, A. S.; Hancock, R. D.; Riebenspies, J. H. *J. Chem. Soc., Dalton Trans.* **1997**, *16*, 2831.  
 (25) de Sousa, A. S.; Hancock, R. D. *J. Chem. Soc., Chem. Commun.* **1995**, 415.  
 (26) Hancock, R. D.; de Sousa, A. S.; Walton, G. B.; Riebenspies, J. H. *Inorg. Chem.* **2007**, *46*, 4749.  
 (27) Hay, B. P.; Zhang, D.; Rustad, J. R. *Inorg. Chem.* **1996**, *35*, 2650–2658.  
 (28) Izatt, R. M.; Pawlak, K.; Bradshaw, K. S.; Bruening, R. L. *Chem. Rev.* **1991**, *91*, 1721.  
 (29) Izatt, R. M.; Pawlak, K.; Bradshaw, K. S.; Bruening, R. L. *Chem. Rev.* **1995**, *95*, 2529.  
 (30) Izatt, R. M.; Terry, R. E.; Haymore, B. L.; Hansen, L. D.; Dalley, N. K.; Avondet, A. G.; Christensen, J. J. *J. Am. Chem. Soc.* **1976**, *98*, 7620–7626.  
 (31) *Cambridge Structural Database*, 5.30 (updated); CCDC: Cambridge, U.K., 2008.

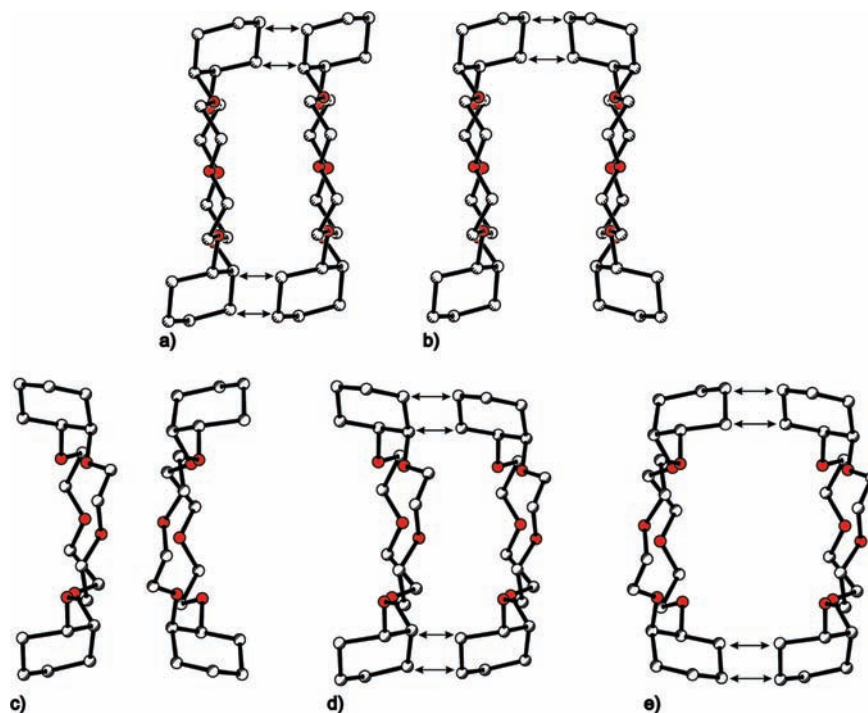


**Figure 1.** Ligand orientations of the *cis-anticyclic* (*a, b*) and *cis-syn-cis* (*c, d, e*) isomers of dicyclohexo-18-crown-6 (REFCODES: CUKZEN and FILDIN<sup>31</sup>) across a Hg–Hg bond for a symmetric dimercury(I) complex. Steric interactions represented by arrows. Hydrogen atoms and metal ion excluded for clarity.

reducing agent, and the crystallization of the symmetric dimercury(I) complex of 18-crown-6 from an alcoholic solution<sup>32</sup> requires the serendipitous reduction of the mercuric salt; potentially significant in sensing of mercury species using small-molecule fluorescent chemosensors.<sup>1,10,33–52</sup>

Elevated temperatures promote the reduction of Hg<sup>2+</sup> to Hg, and hydrothermal syntheses of mercury complexes are infrequent. Polymeric mercuric complexes with phosphorus ylides have been synthesized, using traditional solution methods under ambient conditions, from a methanolic solution of mercuric nitrate in which chelating nitrate anions bridge adjacent mercuric complexes to form a one-dimensional polymeric chain.<sup>53</sup> Milder thermal gradient conditions, employing the branched tube method, are reported to be a useful technique in the synthesis of polymeric mercury coordination complexes with organic ligands.<sup>54,55</sup> Mercury selenoarsenates have, however, been isolated under hydrothermal conditions in which Hg<sup>2+</sup>, in a distorted trigonal planar or tetrahedral geometry,<sup>56</sup> is accommodated within a one-dimensional framework. The hydrothermal synthesis is investigated in this publication with a view to form polymeric chains of the dimercury(I) 18-crown-6 complex.

## Experimental Section

**Materials and General Remarks.** The 18-crown-6 (99%), Mercury(II) nitrate monohydrate (>98%) and Mercury(II) perchlorate hydrate (99.998%) were used as purchased from Alfa Aesar and Aldrich, respectively. Deionized water and *n*-butanol were used for preparation of metal and ligand solutions, respectively. A PTFE-lined Parr autoclave reactor (23 mL) was used for loading of reactants. Hydrothermal syntheses were conducted by placing the autoclave reactor into a temperature controlled drying oven (Fischer Scientific).

- (32) Panda, S.; Singh, H. B.; Butcher, R. J. *Inorg. Chem.* **2004**, *43*, 8532–8537.  
 (33) Huang, W.; Song, C.; He, C.; Lv, G.; Hu, X.; Zhu, X.; Duan, C. *Inorg. Chem.* **2009**, *48*, 5061–5072.  
 (34) Lu, H.; Xiong, L.; Liu, H.; Yu, M.; Shen, Z.; Li, F.; You, X. *Org. Biomol. Chem.* **2009**, *7*, 2554–2558.  
 (35) Choi, M. G.; Kim, Y. H.; Namgoong, J. E.; Chang, S.-K. *Chem. Commun.* **2009**, 3560–3562.  
 (36) Suresh, M.; Mishra, S.; Mishra, S. K.; Suresh, E.; Mandal, A. K.; Shrivastav, A.; Das, A. *Org. Lett.* **2009**, *11*, 2740–2743.  
 (37) Shiraishi, Y.; Sumiya, S.; Kohno, Y.; Hirai, T. *J. Org. Chem.* **2008**, *73*, 1538–1540.  
 (38) Wu, D.; Huang, W.; Duan, C.; Lin, Z.; Meng, Q. *Inorg. Chem.* **2007**, *46*, 1538–1540.  
 (39) Chen, X.; Nam, S.-W.; Jou, M. J.; Kim, Y.; Kim, S.-J.; Park, S.; Yoon, J. *Org. Lett.* **2008**, *10*, 5235–5238.  
 (40) Wu, J.-S.; Hwang, I.-C.; Kim, K. S.; Kim, J. S. *Org. Lett.* **2007**, *9*, 907–910.  
 (41) Coskun, A.; Akkaya, E. U. *J. Am. Chem. Soc.* **2006**, *128*, 607–609.  
 (42) Coskun, A.; Yilmaz, M. D.; Akkaya, E. U. *Org. Lett.* **2007**, *9*, 607–609.  
 (43) Yuan, M.; Li, Y.; Li, J.; Li, C.; Liu, X.; Lv, J.; Xu, J.; Liu, H.; Wang, S.; Zhu, D. *Org. Lett.* **2007**, *9*, 2313–2316.  
 (44) Nolan, E. M.; Lippard, S. J. *J. Am. Chem. Soc.* **2007**, *129*, 5910–5918.  
 (45) Park, S. M.; Kim, M. H.; Choe, J.-I.; No, K. T.; Chang, S.-K. *J. Org. Chem.* **2007**, *72*, 3550–3553.  
 (46) Ho, I.-T.; Lee, G.-H.; Chung, W.-S. *J. Org. Chem.* **2007**, *72*, 2434–2442.  
 (47) Praveen, L.; Ganga, V. B.; Thirumalai, R.; Sreeja, T.; Reddy, M. L. P.; Varma, R. L. *Inorg. Chem.* **2007**, *46*, 6277–6282.  
 (48) Ou, S.; Lin, Z.; Duan, C.; Zhang, H.; Bai, Z. *Chem. Commun.* **2006**, 4392–4394.  
 (49) Nolan, E. M.; Lippard, S. J. *Chem. Rev.* **2008**, *108*, 3443–3480.  
 (50) Czarnik, A. W. *Chem. Biol.* **1995**, *2*, 423–428.  
 (51) de Silva, A. P.; Gunaratne, H. Q. N.; Gunnlaugsson, T.; Huxley, A. J. M.; McCoy, C. P.; Rademacher, J. T.; Rice, T. E. *Chem. Rev.* **1997**, *97*, 1515–1566.  
 (52) de Silva, A. P.; Fox, D. B.; Huxley, A. J. M.; Moody, T. S. *Coord. Chem. Rev.* **2000**, *205*, 41–57.

(53) Sabounchei, S. J.; Nemattalab, H.; Khavasi, H. R. *J. Organomet. Chem.* **2007**, *692*, 54440–5446.

(54) Mahmoudi, G.; Morsali, A.; Zhu, L.-G. *Polyhedron* **2007**, *26*, 2885–2893.

(55) Mahmoudi, G.; Morsali, A. *Polyhedron* **2008**, *27*, 1070–1078.

(56) Chou, J.-H.; Kanatzidis, M. G. *J. Solid State Chem.* **1996**, *123*, 115–122.

**Preparation of  $[\text{Hg}_2(\text{18-crown-6})_2(\text{H}_2\text{O})_2](\text{ClO}_4)_2$  1.** A 0.0033 M solution of 18-crown-6 was prepared by dissolving the compound (0.0440 g, 0.166 mmol) in 50 mL of *n*-butanol. A 0.0033 M solution of  $\text{Hg}(\text{ClO}_4)_2 \cdot (\text{H}_2\text{O})_3$  was prepared at pH 1, through acidification using 1.0 M  $\text{HClO}_4$ , by dissolving (0.0756 g, 0.166 mmol) of the metal salt in 50 mL of deionized water. An aqueous layer (20 mL) of the 0.0033 M metal solution was pipetted into a 50 mL beaker above which the alcoholic solution (20 mL) was carefully introduced with minimal turbulence. Slow evaporation through perforated parafilm afforded off white crystals at the interface over several weeks. The yield for this reaction was 0.0714 g (89.1% based on 18-crown-6). Anal. Calcd (found) for **1**,  $\text{C}_{24}\text{H}_{56}\text{O}_{24}\text{Cl}_2\text{Hg}_2$ : C, 24.01 (23.99), H, 4.70 (4.39). Selected IR data (crystalline solid  $\text{cm}^{-1}$ ): 3554(w), 3488(w), 2916(w), 2887(w), 1621(w), 1463(w), 1435(m), 1353(m), 1286(w), 1252(m), 1072(s), 957(s), 834(s), 746(br, m), 622(s).

**Preparation of  $[\text{Hg}(\text{18-crown-6})](\text{NO}_2)_2$  2.**  $\text{Hg}(\text{NO}_3)_2$  (0.500 g, 1.54 mmol), 18-crown-6 (0.500 g, 1.89 mmol) and 3 mL of 1.0 M  $\text{HNO}_3$  were loaded into a PTFE-lined Parr autoclave. The Parr reactor was heated from ambient temperature to 180 °C over a 3 h period and then soaked for an additional 21 h prior to cooling to ambient conditions. After cooling a transparent pale gray crystalline product was isolated. The yield for this reaction was 0.1736 g (20.24% based on total Hg). Anal. Calcd (found) for **2**,  $\text{C}_{12}\text{H}_{24}\text{N}_2\text{O}_{10}\text{Hg}$ : C, 19.03 (18.66), H, 3.19 (2.84), N, 3.70 (3.50). Selected IR data (crystalline solid  $\text{cm}^{-1}$ ): 2887(w), 2850(w), 1454(w), 1429(m), 1345(m), 1326(w), 1284(m), 1243(m), 1096(s), 960(s), 834(s), 778(w).

### Molecular Structure Determination

**Compound 1,  $[\text{Hg}_2(\text{18-crown-6})_2(\text{H}_2\text{O})_2](\text{ClO}_4)_2$ .** Intensity data were collected on a Bruker APEX II CCD area detector diffractometer with graphite monochromated  $\text{Mo } K_\alpha$  radiation (50 kV, 30 mA) using the APEX 2<sup>57</sup> data collection software. The collection method involved  $\omega$ -scans of width 0.5° and 512 × 512 bit data frames. Data reduction was carried out using the program SAINT+,<sup>58</sup> and face indexed absorption corrections were made using the program XPREP.<sup>58</sup>

The crystal structure was solved by direct methods using SHELXTL.<sup>59</sup> Non-hydrogen atoms were first refined isotropically followed by anisotropic refinement by full matrix least-squares calculations based on  $F^2$  using SHELXTL. Hydrogen atoms were first located in the difference map then positioned geometrically and allowed to ride on their respective parent atoms. Water hydrogen atoms,  $\text{H}_{1\text{WA}}$ ,  $\text{H}_{1\text{WB}}$ ,  $\text{H}_{2\text{WA}}$ , and  $\text{H}_{2\text{WB}}$ , were placed from the difference map and made to ride on their respective parent atoms. Diagrams and publication material were generated using SHELXTL, PLATON,<sup>60</sup> and ORTEP-3.<sup>61</sup>

**Compound 2,  $[\text{Hg}(\text{18-crown-6})](\text{NO}_2)_2$ .** A Bruker SMART 1K diffractometer using the omega scan mode, was employed for crystal screening, unit cell determination, and data collection at 110(2) K. The structures were solved by direct methods, and refined to convergence.<sup>62</sup>

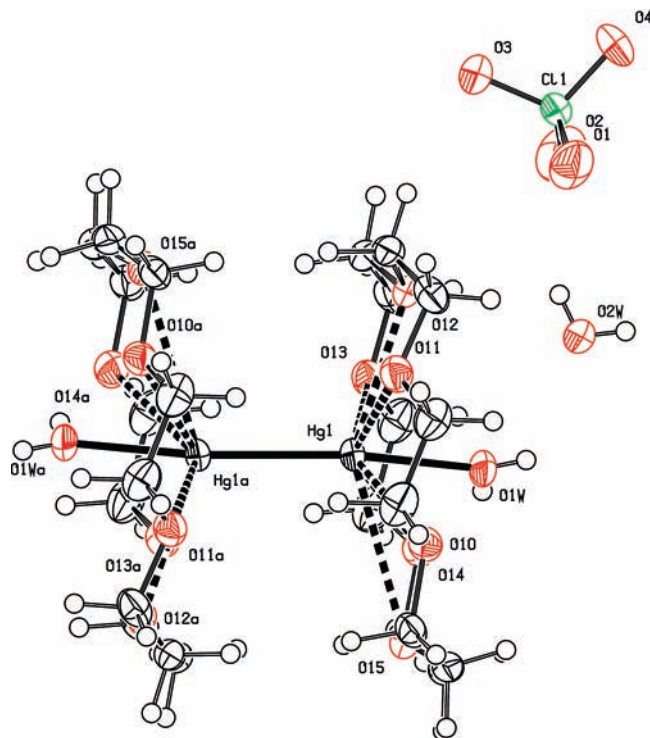


**Figure 2.** ORTEP diagram of the complex  $[(\text{18-crown-6})_2\text{Hg}_2(\text{H}_2\text{O})_2](\text{ClO}_4)_2$ , compound **1**, showing the numbering scheme. Thermal ellipsoids are shown at the 50% probability level.

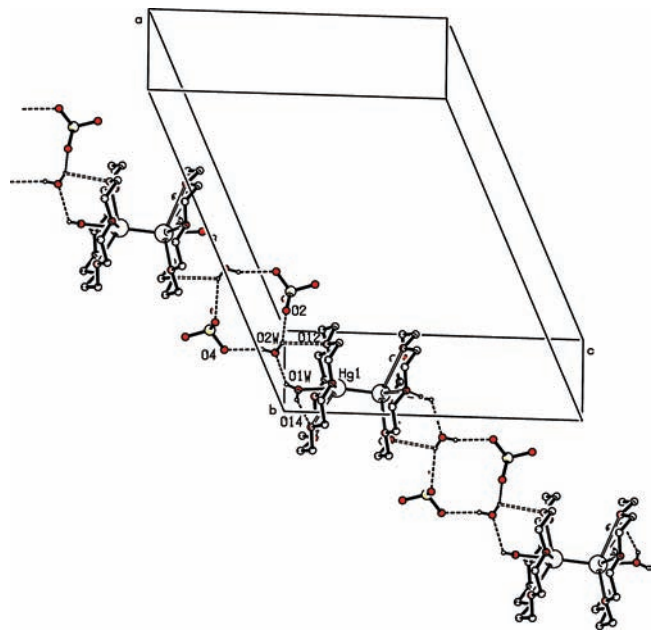


**Figure 3.** Diagram of hydrogen bonding array in  $[(\text{18-crown-6})_2\text{Hg}_2(\text{H}_2\text{O})_2](\text{ClO}_4)_2$ , compound **1**, viewed along  $[1\ 0\ 1]$ .

Absorption corrections were made using the SADABS program.<sup>63</sup> All hydrogens were located in difference Fourier maps (including those at ideal positions).

### Results and Discussion

The first example of a symmetric macrocyclic mercurous complex,  $[\text{L}_2\text{Hg}_2]^{2+}$ , is isolated from an acidic aqueous

(57) Bruker APEX2, Version 2.0-1; Bruker AXS Inc.: Madison, WI, 2005.

(58) Bruker SAINT-NT (includes XPREP and SADABS), Version 6.0; Bruker AXS Inc.: Madison, WI, 2005.

(59) Bruker SHELXTL (includes XS, XL, XP, XSHELL), Version 5.1; Bruker AXS Inc.: Madison, WI, 1999.

(60) Spek, A. L. *J. Appl. Crystallogr.* **2003**, *36*, 7–13.

(61) Farrugia, L. J. *J. Appl. Crystallogr.* **1997**, *30*, 565.

(62) Gabe, E. J.; Le Page, Y.; Charland, J.-P.; Lee, F. L.; White, P. S. *J. Appl. Crystallogr.* **1989**, *22*, 384.

(63) Gorbitz, C. H. *Acta Crystallogr.* **1999**, *B55*, 1090.

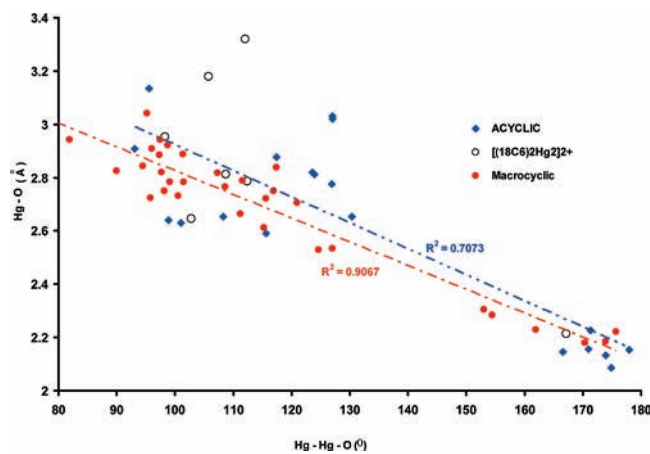


**Figure 4.** Plot of Hg–O distance versus Hg–Hg–O angle for macrocyclic and acyclic mercury complexes bearing a Hg–Hg–O unit.

solution. Repeating the synthesis under hydrothermal conditions afforded a mercuric nitrite complex of 18-crown-6, (Figure 7, Table 2); an unanticipated result considering the thermal and photochemical instability of mercuric nitrite at ambient conditions.<sup>64,65</sup> A recent NMR study on a dimercury(I) asymmetric crown ether complex<sup>19</sup> prompted this study, which reports the isolation of the first symmetric dimercury(I) complex of 18-crown-6 (Figure 2, Table 2). Slow evaporation of a dilute acidic aqueous solution gave the complex  $[(18\text{-crown-6})_2\text{Hg}_2(\text{H}_2\text{O})_2](\text{ClO}_4)_2$  in crystalline form. The resolved structure illustrates a  $D_{3d}$  conformation for the 18-crown-6 macrocycle in the dimercury(I) cation with a Hg–Hg bond length of 2.524(1) Å, that compares favorably with distances observed in solid hydrates. However, Hg–O bond lengths observed for axially coordinated water molecules are larger when compared to the diaqua ion as a consequence of the hydrogen bonding arrays of which they form an integral part. Two short O–H···O interactions are defined by the axially coordinated water molecule, acting as a hydrogen donor via  $\text{H}_{1\text{WB}}$  to an etheral oxygen atom ( $\text{O}_{14}$ ) of the macrocycle and via  $\text{H}_{1\text{WA}}$  to oxygen atom ( $\text{O}_{2\text{w}}$ ) of a proximal solvent water molecule included in the lattice (Figure 3). Oxygen atom ( $\text{O}_{2\text{w}}$ ) further acts as a hydrogen donor to macrocyclic oxygen  $\text{O}_{12}$ , extending the hydrogen bonding array. The angle between the molecular plane of the axially coordinated water molecule and that defined by the macrocyclic oxygen donor atoms, ( $86.8^\circ$ ), suggests that the macrocyclic cavity and the axially coordinated water molecule are orthogonally related. The  $\text{Hg}_{1\text{a}}\text{--Hg}_1\text{--O}_{1\text{w}}$  angle ( $167.05^\circ$ ) strongly suggests the above-mentioned O–H···O interactions bend the O–Hg–Hg–O unit, often observed in salts of mercurous complexes as essentially linear.

Hg–O bond lengths to axially coordinated water molecules, describing the quasi-linear  $\text{H}_2\text{O--Hg--Hg--OH}_2$  unit are notably shorter than distances to macrocyclic oxygen atoms of 18-crown-6 (Table 3). Short bonds to mercury defining structural linearity, equally common in several mercuric complexes of 18-crown-6, are attributed to relativistic effects<sup>66</sup> and the preferential formation of sp hybrid orbitals for mercury.

The predominance of linear coordination geometries in macrocyclic and acyclic dimercury(I) complexes comprising

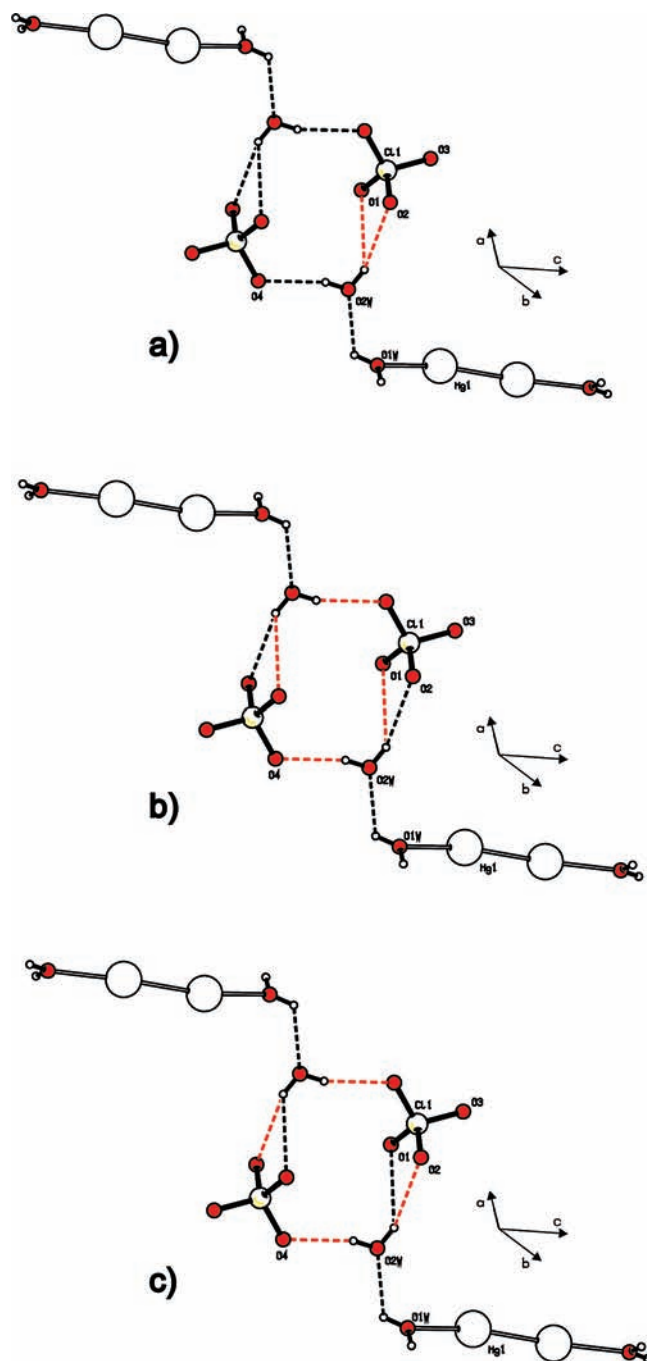


**Figure 5.** Hydrogen bonding motifs described by the O–H···O interactions between perchlorate anions and lattice water molecules in compound 1. (a) Bifurcated  $\text{O}_{2\text{w}}\text{--H}_{2\text{WB}}\cdots\text{O}$  interaction;  $\text{O}_{2\text{w}}$  interacts as a hydrogen donor via  $\text{H}_{2\text{WB}}$  to perchlorate oxygens  $\text{O}_1$  and  $\text{O}_2$  defining a  $R_2^2(4)$  motif. (b)  $R_2^2(12)$  motif described by the  $\text{O}_{2\text{w}}\text{--H}\cdots\text{O}$  interaction between  $\text{O}_{2\text{w}}$  as a hydrogen donor to perchlorate oxygen atoms  $\text{O}_1$  via  $\text{H}_{2\text{WB}}$  and  $\text{O}_4$  via  $\text{H}_{2\text{WA}}$ . (c)  $R_2^2(12)$  motif described by the  $\text{O}_{2\text{w}}\text{--H}\cdots\text{O}$  interaction between  $\text{O}_{2\text{w}}$  as a hydrogen donor to perchlorate oxygen atoms,  $\text{O}_2$  via  $\text{H}_{2\text{WB}}$  and  $\text{O}_4$  via  $\text{H}_{2\text{WA}}$ .

a quasi-linear Hg–Hg–O unit is graphically illustrated by the inverse relationship between Hg–O contact distance or bond length and Hg–Hg–O angle (Figure 4). Least-squares lines have been independently fitted to relationships for macrocyclic and acyclic complexes using Excel<sup>67</sup> which facilitates the calculation of coefficients of determination ( $R^2$ ).

(64) Ray, P. C. *J. Chem. Soc., Trans.* **1905**, 87, 171–177.

(65) Potts, R. A.; Allred, A. L. *Inorg. Chem.* **1966**, 5, 1066–1071.

(66) Hancock, R. D.; Reibenspies, J. H.; Maumela, H. *Inorg. Chem.* **2004**, 43, 2981–2987.

(67) Billo, E. J. *Excel for Chemists*; Wiley-VCH: New York, 2001.

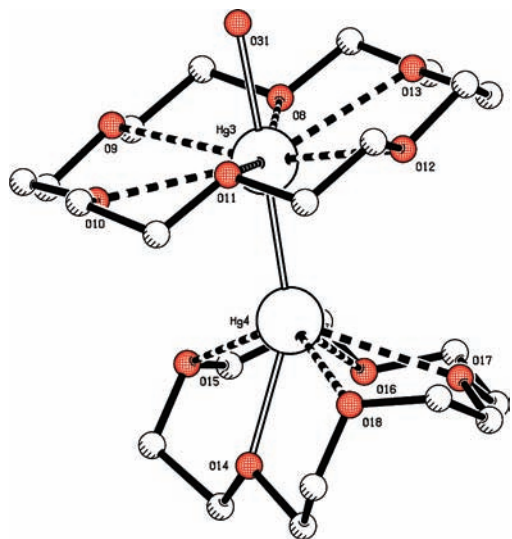


**Figure 6.** Asymmetric dimercury(I) complex showing a highly distorted conformation of 15-crown-5 as reported by Peringer and co-workers.<sup>19</sup> Hydrogen atoms and disordered molecules removed for clarity.

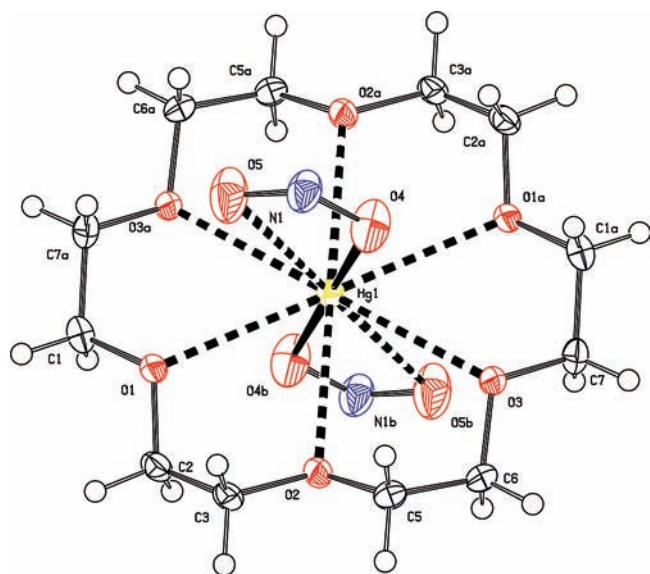


**Figure 7.** ORTEP diagram of [(18-crown-6)Hg](NO<sub>2</sub>)<sub>2</sub>, compound 2, showing the numbering scheme. Thermal ellipsoids are shown at the 50% probability level.

The  $R^2$  value for the macrocyclic plot is better than 0.9 and drops substantially to 0.7 for acyclic complexes. Current solid state data for macrocyclic dimercury(I) complexes consists of three structures including the structure reported here (Figure 2). In macrocyclic complexes shorter mercury to oxygen distances (2.1–2.4 Å) define Hg–O bonds to oxygen atoms of axially coordinated ligands. Variations in bond angle for these Hg–O bonds are inevitably associated with hydrogen bonding to solvent molecules included in the lattice or counterions in the immediate proximity. Asymmetric bidentate chelation of acyclic analogues have a similar effect and result in moderate scatter of plotted points. Longer mercury to oxygen distances (Hg–O > 2.4 Å), indicative of van der Waals type interactions, are observed for oxygen donors in macrocyclic backbones and acyclic multidentate chelating ligands. Asymmetric and out-of-plane chelation relative to the Hg–Hg bond in acyclic dimercury(I)

**Table 2.** Crystallographic Details for [Hg<sub>2</sub>(18-crown-6)<sub>2</sub>(H<sub>2</sub>O)<sub>2</sub>](ClO<sub>4</sub>)<sub>2</sub> (**1**) and [Hg(18-crown-6)](NO<sub>2</sub>)<sub>2</sub> (**2**)

	C <sub>24</sub> H <sub>56</sub> Cl <sub>2</sub> Hg <sub>2</sub> -O <sub>24</sub> ( <b>1</b> )	C <sub>12</sub> H <sub>24</sub> Hg N <sub>2</sub> O <sub>10</sub> ( <b>2</b> )
empirical formula	C <sub>24</sub> H <sub>56</sub> Cl <sub>2</sub> Hg <sub>2</sub> -O <sub>24</sub> ( <b>1</b> )	C <sub>12</sub> H <sub>24</sub> Hg N <sub>2</sub> O <sub>10</sub> ( <b>2</b> )
formula weight	1200.77	556.92
temperature (K)	173(2)	110(2) K
wavelength (Å)	0.71073	0.71073
crystal system	monoclinic	monoclinic
space group	C2/c	P2(1)/c
<i>a</i> (Å)	21.0345(9)	8.027(5)
<i>b</i> (Å)	12.1565(5)	14.473(9)
<i>c</i> (Å)	16.8010(7)	7.827(5)
$\beta$ (deg)	113.2000(10)	95.165(11)
volume (Å <sup>3</sup> )	3948.7(3)	905.6(10)
<i>Z</i>	4	2
density (calculated) (Mg m <sup>-3</sup> )	2.020	2.042
Absorption coefficient (mm <sup>-1</sup> )	7.987	8.550
<i>F</i> (000)	2344	540
crystal size (mm)	0.32 × 0.29 × 0.22	0.20 × 0.20 × 0.10
$\theta$ range for data collection (deg)	1.98–28.00	2.81–25.00
limiting indices	–27 < <i>h</i> < 27 –16 < <i>k</i> < 16 –22 < <i>l</i> < 22	–9 < <i>h</i> < 9 –17 < <i>k</i> < 17 –9 < <i>l</i> < 9
reflections collected/unique	30784/4760	6822/1557
<i>R</i> <sub>int</sub>	0.0593	0.0340
completeness to $\theta = 28.00^\circ$	100.0%	97.4%
data/restraints/parameters	4760/0/235	1557/0/115
goodness of fit <i>F</i> <sup>2</sup>	1.048	1.003
final <i>R</i> indices [ <i>I</i> > 2 $\sigma$ ( <i>I</i> )]	<i>R</i> 1 = 0.0234, w <i>R</i> 2 = 0.0584	<i>R</i> 1 = 0.0175, w <i>R</i> 2 = 0.0430
<i>R</i> indices (all data)	<i>R</i> 1 = 0.0288, w <i>R</i> 2 = 0.0604	<i>R</i> 1 = 0.0214, w <i>R</i> 2 = 0.0466
largest differential peak and hole (e Å <sup>-3</sup> )	3.161 and –0.949	0.748 and –0.862

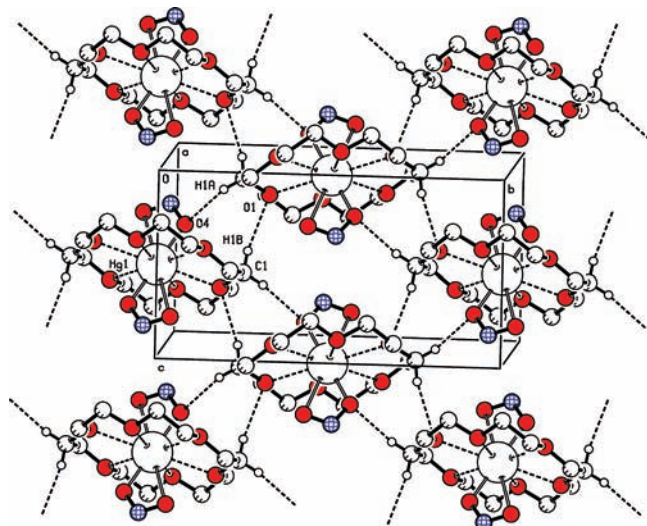
**Table 3.** Hg–O Distances and Bond lengths in [Hg<sub>2</sub>(18-crown-6)<sub>2</sub>(H<sub>2</sub>O)<sub>2</sub>](ClO<sub>4</sub>)<sub>2</sub> (**1**) and [Hg(18-crown-6)](NO<sub>2</sub>)<sub>2</sub> (**2**)

bond	Hg–O distance	bond length (Å)	oxygen type
( <b>1</b> )			
Hg <sub>1</sub> –O <sub>15</sub>	3.181(2)		(etheral, macrocyclic)
Hg <sub>1</sub> –O <sub>14</sub>	3.320(2)		(etheral, macrocyclic)
Hg <sub>1</sub> –O <sub>13</sub>	2.951(2)		(etheral, macrocyclic)
Hg <sub>1</sub> –O <sub>12</sub>	2.809(2)		(etheral, macrocyclic)
Hg <sub>1</sub> –O <sub>10</sub>	2.786(2)		(etheral, macrocyclic)
Hg <sub>1</sub> –O <sub>11</sub>		2.644(2)	(etheral, macrocyclic)
Hg <sub>1</sub> –O <sub>1w</sub>		2.205(2)	(aqua, axial coordination)
( <b>2</b> )			
Hg <sub>1</sub> –O <sub>1</sub>	2.816(2)		(etheral, macrocyclic)
Hg <sub>1</sub> –O <sub>2</sub>	2.782(3)		(etheral, macrocyclic)
Hg <sub>1</sub> –O <sub>3</sub>	2.880(2)		(etheral, macrocyclic)
Hg <sub>1</sub> –O <sub>4</sub>		2.122(3)	(nitrito)
Hg <sub>1</sub> –O <sub>5</sub>	2.798(3)		(nitrito)

complexes leads to substantial variation in Hg–Hg–O angles resulting in the observed drop in  $R^2$  for the least-squares fit of acyclic complexes. Oxygen donors in macrocyclic crown ethers are, however, restricted by a less flexible macrocyclic backbone, 18-crown-6 tending toward the preferred  $D_{3d}$  conformation adopted for complexation of metal ions. Hg–Hg–O angles associated with the oxygen donor

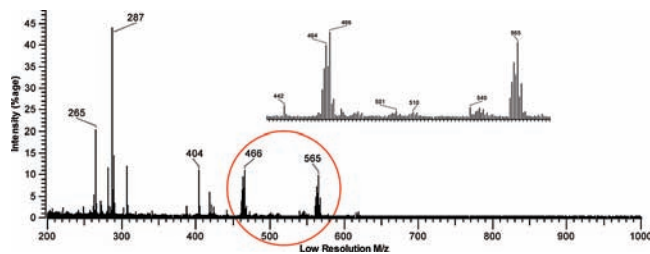
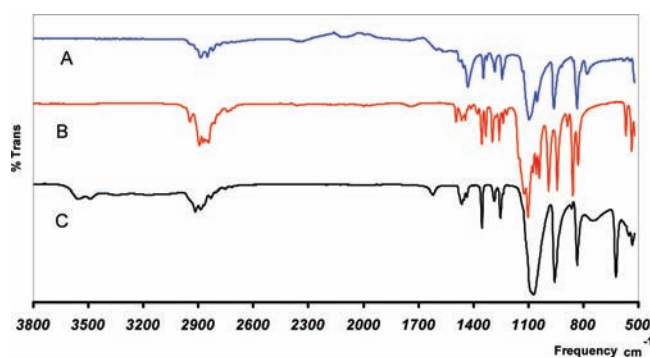
**Table 4.** Hydrogen Bonding Motifs in  $[\text{Hg}_2(18\text{-crown-6})_2(\text{H}_2\text{O})_2](\text{ClO}_4)_2$  (**1**) for Included Solvent Water Molecules and Perchlorate Ions

D–H	$d(\text{D–H})$	$d(\text{H}\cdots\text{A})$	DHA	$d(\text{D}\cdots\text{A})$	A	symmetry
$\text{O}_{2\text{W}}\text{–H}_{2\text{WB}}$	0.863	2.306	163.70	3.143	O2	$[x, y, z]$
$\text{O}_{2\text{W}}\text{–H}_{2\text{WB}}$	0.863	2.426	134.93	3.096	O1	$[x, y, z]$
$\text{O}_{2\text{W}}\text{–H}_{2\text{WA}}$	0.866	2.046	159.32	2.872	O4	$[\frac{1}{2} - x,$ $1\frac{1}{2} - y, -z]$

**Figure 8.** Diagram of intermolecular  $\text{C}_1\text{–H}_{1\text{B}}\cdots\text{O}_1$  and  $\text{O}_4\cdots\text{H}_{1\text{A}}\text{–C}_1$  interactions between adjacent layers of compound **2**,  $[(18\text{-crown-6})\text{Hg}](\text{NO}_2)_2$ .

atoms of crown ethers depend on how well the macrocyclic cavity accommodates the mercury ion. The average radius of the macrocyclic cavity for 18-crown-6 is reported as 1.45 Å,<sup>68–71</sup> and a centrally coordinated mercurous ion, ionic radius 1.19 Å,<sup>72</sup> resembling the observed coordination mode of the mercuric ion<sup>12–16,73</sup> might be expected. Structures of crown ether dimercury(I) complexes<sup>19</sup> show the mercury ion is elevated by approximately 0.4 Å from the plane defined by the donor atoms of 18-crown-6, and as much as 1.23 Å in the case of 15-crown-5, responsible for variation in Hg–Hg–O angles with increasing Hg–O separation.

In the symmetric dimercury(I) complex reported here the mercurous ion is elevated 0.835 Å above the mean plane of oxygen donors that do not encapsulate the metal ion within the macrocyclic cavity. Non-bonding interactions between 18-crown-6 fragments, defined by short hydrogen–hydrogen contacts, translate across a 2-fold axis of symmetry bisecting the Hg–Hg bond. The separation for the non-bonded  $\text{H}\cdots\text{H}$  contacts are 2.11(1) Å between  $\text{H}_{4\text{A}}$  and  $\text{H}_{12\text{A}}$  and 2.33(1) Å between  $\text{H}_{5\text{B}}$  and  $\text{H}_{9\text{B}}$ . These interactions may be deemed short if the van der Waals contact distance for the hydrogen atom is set to a crystallographically determined value of 2.4 Å, arguably overestimated when compared to

**Figure 9.** FAB Mass Spectrum for compound **1**,  $[(18\text{-crown-6})_2\text{Hg}_2(\text{H}_2\text{O})_2](\text{ClO}_4)_2$ , in NBA matrix.**Figure 10.** Solid State IR spectra of  $[(18\text{-crown-6})\text{Hg}](\text{NO}_2)_2$  (A), 18-crown-6 (B), and  $[(18\text{-crown-6})_2\text{Hg}_2(\text{H}_2\text{O})_2](\text{ClO}_4)_2$  (C).

neutron diffraction measurements.<sup>74–76</sup> The short  $\text{H}\cdots\text{H}$  contacts have  $\text{H–C–C–H}$  torsion angles  $129.9(1)^\circ$  and  $175.2(1)^\circ$ , respectively, accommodated via distortion of the  $D_{3d}$  conformation. The mercurous ion is consequently complexed well above the macrocyclic cavity resulting in very long mercury to oxygen distances and subsequent variation in Hg–Hg–O angles involving macrocyclic oxygen donors. The  $R^2$  value for the macrocyclic least-squares fit (Figure 4) drops significantly to 0.75 upon inclusion of solid state data (open circles) for the symmetric dimercury(I) complex of 18-crown-6 (Figure 2), largely because of the longest mercury to oxygen distances observed to date. Extreme limits for Hg–O van der Waals interactions ( $2.73 \text{ \AA}$ <sup>72,77</sup>) can be generously described using the Hg(I) crystal and O van der Waals radii. Interactions between the mercurous ion and ethereal oxygens  $\text{O}_{10}$  and  $\text{O}_{12}$  are expected to be very weak while orientations of  $\text{O}_{13}$ ,  $\text{O}_{14}$ , and  $\text{O}_{15}$  arise primarily from conformational twisting of the crown ether to accommodate the short  $\text{H}\cdots\text{H}$  contacts.

The use of a weakly coordinating anion, such as perchlorate in the proximity of oxygen bearing ligands, further prevents disproportionation of the mercurous ion and

(68) Dalley, N. K.; Izatt, R. M.; Christensen, J. J. *Synthetic and Multidentate Macrocyclic Compounds*; Academic Press: New York, 1978; p 207.

(69) Shannon, R. D.; Prewitt, C. T. *Acta Crystallogr., Sect. B* **1969**, *25*, 925.

(70) Shannon, R. D.; Prewitt, C. T. *Acta Crystallogr., Sect. B* **1970**, *26*, 1046.

(71) Vogtle, F.; Weber, E. *Crown ethers and analogues*; John Wiley & Sons: New York, 1989; pp 208–292.

(72) Shannon, R. D. *Acta Crystallogr.* **1976**, *A* **32**, 751–767.

(73) El Essawi, M.; Abd El Khalik, S.; Tebbe, K.-F. *Acta Crystallogr., Sect. C: Cryst. Struct. Commun.* **1996**, *52*, 818–820.

(74) Baur, W. H. *Acta Crystallogr., B* **1972**, *28*, 1456–1465.

(75) Bondi, A. J. *Chem. Phys.* **1964**, *68*, 441–451.

(76) Lehmann, M. S.; Verbist, J. J.; Hamilton, W. C.; Koetzle, T. F. *J. Chem. Soc., Perkin II* **1973**, 133–137.

(77) Atkins, P. W.; De Paula, J. *Physical Chemistry*, 8th ed.; W. H. Freeman: New York, 2006.

facilitates crystallization. The weakly coordinating nature of the perchlorate counterion is reflected by the disorder observed for the anion in the solid state. Non-bonded interactions, in which the perchlorate oxygen atoms participate as hydrogen acceptors, generate hydrogen bonding arrays that remove the disorder associated with the anion. Included solvent water molecules in the structure of the symmetric 18-crown-6 dimercury(I) complex, stabilizes the uncoordinated perchlorate anion through three O–H···O interactions (Table 4). The water molecule located at  $(x, y, z)$  acts as a hydrogen donor via  $H_{2WB}$  to the perchlorate oxygens  $O_1$  and  $O_2$  at  $(x, y, z)$  to form a bifurcated hydrogen bonding  $R_1^2(4)$  ring motif<sup>78</sup> (Figure 5a). An additional discrete interaction for the same water molecule occurs via  $H_{2WA}$  to perchlorate oxygen  $O_4$  at  $(1/2 - x, 11/2 - y, -z)$  that when combined with either interaction of  $H_{2WB}$  affords a more elaborate  $R_2^4(12)$  ring motif (Figure 5, panels b, c) generated through a center of inversion<sup>78</sup> at  $(1/4, 1/4, 0)$ .

The importance of relativistic effects in crown ether complexes of mercury is easily appreciated when compared to cadmium(II) analogues. The unexpectedly high stability of cadmium(II) complexes with crown ethers has been attributed to the plasticity of this ion's coordination geometries, reflected in their insensitive response toward differences in cavity size.<sup>79</sup> This is well illustrated in cadmium(II) complexes of 15-crown-5 where oxygen donor atoms occupy axial positions.<sup>80,81</sup> The ability of cadmium(II) to modulate equatorial bond lengths in crown ether complexes, because of complete or partial absence of relativistic effects, is unparalleled in mercury complexes in which M–L bonds exhibit high covalence.<sup>82</sup> Relativistic effects prevalent in an asymmetric dimercury(I) complex prepared by Peringer and co-workers<sup>19</sup> cause the unusual conformation of the 15-crown-5 macrocycle, in which oxygen donor  $O_{14}$  is displaced by 1.225 Å from the mean plane defined by the remaining four oxygen donor atoms (Figure 6). The macrocyclic cavity of 15-crown-5 is reported to be 0.92 Å,<sup>68,70,71</sup> smaller than the mercurous ionic radius (1.19 Å),<sup>72</sup> and preempts coordination of the mercurous ion well above (1.31 Å) the plane defined by oxygen donor atoms of 15-crown-5. The  $Hg_4-O_{14}$  bond length (2.304 Å) is substantially shorter than the average Hg–O distance (2.73 Å) for interactions with macrocyclic oxygen donors. It compares favorably with the  $Hg_3-O_{31}$  bond length (2.22 Å) for the axially coordinated water defining a linear Hg–Hg–O unit (175.78°). The  $Hg_3-Hg_4-O_{14}$  bond angle (153.04°) reveals the tendency toward pseudo-linearity compared to the averaged Hg–Hg–O angle (114.12°) for the remaining macrocyclic oxygen donors associated with equatorial sites. In the absence of an axially coordinated water molecule, as observed for the symmetric dimercury(I) complex of 18-crown-6, the preferred linear coordination geometry is accommodated by the 15-crown-5 (Figure 6).

**Hydrothermal Studies.** Attempted hydrothermal synthesis of polymeric mercurous complexes resulted in the

crystallization of the mercuric nitrite complex of 18-crown-6,  $[Hg(18-crown-6)]^{2+}(NO_2^-)_2$ , (Figure 7, Table 2). Solid state study of this complex reveals the pseudorotaxane type structure previously reported for the mercuric nitrate complex,  $[Hg(18-crown-6)]^{2+}(NO_3^-)_2$ .<sup>83</sup> Conformation of the crown ether in the mercuric nitrite complex mimics that observed in the nitrate counterpart, showing no significant distortions from the  $D_{3d}$  conformation. Relativistic effects are evidenced by asymmetric coordination of the nitrite anion exhibiting very short Hg–O bonds (2.122 Å, Table 3). A long Hg–O van der Waals type interaction (2.798 Å, Table 3), further describes the coordination mode of the nitrite anion. Frequency bands for N–O stretching vibrations ( $\nu_1 = 1096\text{ cm}^{-1}$ ,  $\nu_2 = 1429\text{ cm}^{-1}$ ) observed in the solid state IR spectrum (Figure 10) are significantly divergent ( $333\text{ cm}^{-1}$ ), preempting a unidentate nitrito (*cis to metal*) coordination mode.<sup>84,85</sup> Elucidation of nitrate coordination modes using vibrational spectroscopy alone can be misleading. N–O stretching vibrations ( $\nu_1 = 1284\text{ cm}^{-1}$ ,  $\nu_2 = 1510\text{ cm}^{-1}$ ) are observed in the solid state spectrum of the mercuric nitrate complex of 18-crown-6.<sup>83</sup> The separation of the N–O nitrate bands ( $226\text{ cm}^{-1}$ ), suggests a bidentate chelation mode merits consideration.<sup>84</sup> Analyses of Hg–O bond lengths and interaction distances, however, show the nitrate coordination to be more asymmetric than the nitrite. An elongated, (0.02 Å), Hg–O bond length (2.122 Å, Table 3), for the nitrite oxygen atoms is offset by a shortened, (0.085 Å), Hg–O nitrite interaction (2.798 Å, Table 3), causing an overall decrease in mercury to oxygen distances for the nitrito ligand. Orientation of the unidentate nitrate ligand, as defined by an angled alignment of the O–Hg–O unit threading the macrocyclic cavity, is explained by a weak stabilizing CH···O interaction between the macrocyclic backbone and the distant nitrate oxygen. C···O and H···O separations, of 3.13 Å and 2.48 Å, respectively, attribute marginal significance to this weak CH···O interaction. Longer  $C_7\cdots O_5$  and  $H_{7A}\cdots O_5$  distances, of 3.16(1) Å and 2.51(1) Å, respectively, defining an analogous CH···O interaction in the nitrite complex imply the  $C_7-H_{7A}\cdots O_5$  interaction is weaker than the corresponding  $C_6-H_{11}\cdots O_{5B}$  interaction for the nitrate oxygen. Additional weak intermolecular C–H···O interactions, involving the nitrito ligand and the crown ethereal oxygens, describe the formation of layers (Figure 8) parallel to (1, 0, 0). The nitrito oxygen  $O_4$  at  $(x, y, z)$  acts as a hydrogen acceptor via  $H_{1A}$  on carbon  $C_1$  at  $(-x, 1/2 + y, 1/2 - z)$ . Carbon  $C_1$  at  $(x, y, z)$  in turn acts as a hydrogen donor via  $H_{1B}$  to an ethereal oxygen  $O_1$  at  $(x, 1/2 - y, -1/2 + z)$ . A second interaction  $C_6-H_{6A}\cdots O_5$  has an H···O distance equal to 2.931 Å more typical of intermolecular interactions associated with molecular clusters and adducts of 18-crown-6. This C–H···O interaction is significantly larger (0.144 Å) than the corresponding  $C_1-H_{11}\cdots O_{5B}$  interaction observed for the nitrate ligand, a consequence of a more symmetrically coordinated nitrito ligand.

(78) Bernstein, J.; Davis, R. E.; Shinoni, L.; Chang, N. L. *Angew. Chem., Int. Ed. Engl.* **1995**, *34*, 1555–1573.

(79) Harrington, J. M.; Jones, S. B.; White, P. H.; Hancock, R. D. *Inorg. Chem.* **2004**, *43*, 4456–4463.

(80) Bond, A. H.; Rogers, R. D. *J. Chem. Crystallogr.* **1998**, *28*, 521–527.

(81) Braga, D.; Gandolfi, M.; Lusi, M.; Polito, M.; Rubini, K.; Grepioni, F. *Cryst. Growth Des.* **2007**, *7*, 919–924.

(82) Hancock, R. D.; Marsicano, F. *Inorg. Chem.* **1980**, *19*, 2709–2714.

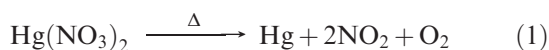
(83) Callega, M.; Steed, J. J. *Chem. Crystallogr.* **2003**, *33*, 609–612.

(84) Nakamoto, K. *Infrared Spectra of Inorganic and Coordination Compounds*, 3rd ed.; Wiley: New York, 1978.

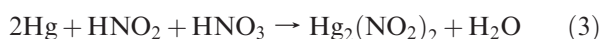
(85) Chattopadhyay, T.; Podder, N.; Banu, K. S.; Banerjee, A.; Ghosh, M.; Suresh, E.; Nethaji, M.; Das, D. *J. Mol. Struct.* **2007**, *839*, 69–75.



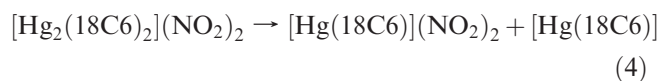
Under ambient conditions the formation of complexes containing nitrogen in lower oxidation states is unlikely given the weak reducing power of mercury species and the strong but slow oxidizing nature of nitrates. However, the hydrothermal synthesis using mercuric nitrate in dilute nitric acid at elevated temperature enhances the reduction of mercury ions to elemental mercury<sup>56</sup> that may accompany the formation of products exhibiting nitrogen in lower oxidation states.<sup>86</sup> Elevated temperature (180 °C) and pressure, coupled with high acidity (pH ≈ 1), enhances the oxidizing power of nitrates and promotes the decomposition of mercuric nitrate to mercury metal and nitrogen dioxide (eq 1). Under hydrothermal conditions the formation of nitrogen dioxide can also be attributed to thermal decomposition of nitric acid (eq 2).



The reaction of nitrogen dioxide with water affords equimolar mixtures of nitric and nitrous acid reported to play a vital role in the dissolution of mercury metal.<sup>64,87</sup> Although itself susceptible to disproportionation, nitrous acid is a strong oxidizing agent. It plays a catalytic role in the dissolution of metals accounting for the initially preferred formation of mercurous nitrite, a yellow crystalline solid, that undergoes decomposition spontaneously under ambient conditions.<sup>65</sup> Early studies on the action of dilute nitric acid upon elemental mercury report the formation of mercurous nitrite almost exclusively (eq 3) followed by gradual formation of unstable mercurous nitrate upon evaporation,<sup>64,87</sup> reported to decompose rapidly upon heating with the evolution of nitrogen dioxide.<sup>65</sup>



In hot aqueous solution, mercurous nitrite is known to disproportionate slowly (approximately 20%) to mercuric nitrite and mercury.<sup>64</sup> The former may be stabilized through complexation by the crown ether forming the observed product. This mechanism proposes that disproportionation, affording mercuric nitrite, occurs prior to the complexation of the metal ion and precludes the formation of the 18-crown-6 dimercury(I) complex,  $[\text{Hg}_2(18\text{-crown-6})_2]^{2+}(\text{NO}_2^-)_2$ . An alternative mechanism permits the formation of the 18-crown-6 dimercury(I) complex, enjoying enhanced stability as a result of the shift in the disproportionation equilibrium caused by elemental mercury originating from the reduction of the mercuric nitrate. Complexation of the dimeric mercurous ion now precedes disproportionation of the dimercury(I) complex, yielding the mercuric nitrite complex, compound **2**, and a neutral mercury complex (eq 4).



The latter explanation for the isolation of compound **2** is more credible given the instability of mercuric nitrite noted under ambient conditions. The possibility of compound **2** originating from the dimercury(I) nitrate complex,  $[\text{Hg}_2(18\text{-crown-6})_2]^{2+}(\text{NO}_3^-)_2$ , in which the dimercury(I) complex acts as a reductant, is unlikely given that the mechanism for two electron oxidants exhibits an inverse dependence upon the mercuric ion.<sup>88</sup>

FAB-source mass spectrometry of compound **1** (Figure 9) in a nitrobenzyl alcohol (NBA) matrix suggests disproportionation and/or Hg–Hg bond cleavage give rise to the observed species. Homolytic cleavage of the Hg–Hg bond affords a mercurous complex,  $[(18\text{-crown-6})\text{Hg}]^+$ , resulting in the observed cluster of peaks centered at  $m/z$  466. Heterolytic cleavage, indistinguishable from disproportionation, results in the formation of a neutral mercury complex,  $[\text{Hg}(18\text{-crown-6})]$ , and a mercuric complex,  $[(18\text{-crown-6})\text{Hg}]^{2+}$ , observable as a mono cationic species,  $[(18\text{-crown-6})\text{Hg}]^{2+}(\text{ClO}_4)^-$ , centered at  $m/z$  565. FAB-mass spectrometry on a mercuric complex of 18-crown-6 indicates mercuric ions remain complexed by the crown ether under experimental conditions.<sup>13</sup> Density-functional theory (DFT) calculations strongly suggest dissociation becomes possible when the required macrocyclic cavity size, such as that calculated for the neutral mercury complex,  $[\text{Hg}(18\text{-crown-6})]$ , significantly exceeds cavity sizes observed in cationic complexes of mercury or in free 18-crown-6.<sup>89</sup> Peaks at  $m/z$  287 and 265 correspond to the  $\text{Na}^+$  complex of 18-crown-6,  $[\text{Na}(18\text{-crown-6})]^+$ , and protonated crown ether,  $[\text{H}(18\text{-crown-6})]^+$ , respectively, for which dissociation of existing mercury complexes is a prerequisite. Dissociation of the unobservable neutral mercury complex may contribute significantly, although not exclusively, to the availability of free 18-crown-6 for complexation of a proton or sodium ion in the ionization process.

**Infra Red Studies.** Theoretical studies elucidating vibration modes of 18-crown-6<sup>90,91</sup> and that of its complexes<sup>92–94</sup> appear in the literature. Stretching  $\text{CH}_2$  modes for the oxyethylene backbone of the crown ether observed in the 2800 to 2900  $\text{cm}^{-1}$  region are not exploited for investigating complexation in aqueous solution. These vibration modes can be obscured by broad O–H bands arising from solvent interactions or interaction with hydrogen bonded species, and are subject to little variation upon complexation. Frequencies in 1500 to 1200  $\text{cm}^{-1}$  and 1100 to 800  $\text{cm}^{-1}$  regions are responsive toward inclusion of metal ions in the macrocyclic cavity and exhibit significant changes observable by IR spectroscopy for hydrogen bonded species. The former comprises  $\text{CH}_2$  oscillations defined by scissoring (1500 to 1400  $\text{cm}^{-1}$ ), wagging (1390 to 1300  $\text{cm}^{-1}$ ), and bending (1300 to 1200  $\text{cm}^{-1}$ ) modes of the macrocycle in this established

(88) Davies, R.; Kipling, R.; Sykes, A. G. *J. Am. Chem. Soc.* **1973**, *95*, 7250–7256.

(89) Bagatur'yants, A. A.; Freidzon, A. Y.; Alfimov, M. V.; Baerends, E. J.; Howard, J. A. K.; Kuz'mina, L. G. *J. Mol. Struct.* **2002**, *588*, 55–69.

(90) Fukuhara, K.; Ikeda, K.; Matsuura, H. *J. Mol. Struct.* **1990**, *224*, 203–224.

(91) Al-Khatani, A. A. *Spectrochimica Acta, Part A* **2002**, *58*, 2877–2884.

(92) Chenevert, R.; Rodrigue, A.; Chamberland, D.; Ouellet, J.; Savoie, R. *J. Mol. Struct.* **1985**, *131*, 187–200.

(93) Gjikaj, M. *Vib. Spectrosc.* **2005**, *39*, 262–265.

(94) Mosier-Boss, P. A. *Spectrochim. Acta, Part A* **2005**, *61*, 527–534.

(86) Fanning, J. C. *Coord. Chem. Rev.* **2000**, *199*, 159–179.

(87) Ray, P. C. *J. Chem. Soc., Trans.* **1897**, *71*, 337–345.

order. Bands in the latter region are associated with deformities in the macrocyclic backbone in the immediate vicinity of ethereal oxygens. Changes in bond angles involving the oxygen donors are also reported to affect bands observed at frequencies between 600 and 500  $\text{cm}^{-1}$ . The regular conformation of  $D_{3d}$  symmetry adopted by the crown ether in compound **1**, [(18-crown-6) $_2$ Hg $_2$ (H $_2$ O) $_2$ (ClO $_4$ ) $_2$ ], and compound **2**, [(18-crown-6)Hg](NO $_2$ ) $_2$ ], is deduced from a direct comparison between their solid state IR spectra with that of uncomplexed 18-crown-6 (Figure 10). Distortions of the free, uncomplexed crown ether result in appreciable splitting of vibrational modes (Spectrum B, Figure 10) more easily observed for frequencies between 1000 and 800  $\text{cm}^{-1}$ . Bands observed at 991, 946, 857, and 827  $\text{cm}^{-1}$  (Spectrum B, Figure 10) are replaced by broader intense bands at 957 and 834  $\text{cm}^{-1}$  (Spectrum C, Figure 10) in compound **1** and at 960 and 834  $\text{cm}^{-1}$  (Spectrum A, Figure 10) in compound **2**. Absence of splitting is also evident at frequencies corresponding to CH $_2$  scissoring, wagging, and bending vibrational modes. Bond angle (C–O–C) deformations observed at 569 and 536  $\text{cm}^{-1}$  (Spectrum B, Figure 10) are largely absent in spectra of compounds **1** and **2** (Spectra A and C, Figure 10) indicative of the regular crown orientation expected for the  $D_{3d}$  conformer. The intense band at 622  $\text{cm}^{-1}$  (Spectrum C, Figure 10) is assigned to C–O–C bond angle deformations involving ethereal oxygens O $_{12}$  and O $_{15}$ . Bond angles C $_{10}$ –O $_{15}$ –C $_{11}$  and C $_5$ –O $_{12}$ –C $_4$  of 111.2° and 111.7°, respectively, represent the greatest deviations from the average C–O–C bond angle (112.5°)<sup>30</sup> in 18-crown-6 conformations. We identified short non-bonded H···H contacts to rationalize the distortion of the  $D_{3d}$  conformation in compound **1** present in oxyethylene fragments C $_9$ –C $_{10}$ –O $_{15}$ –C $_{11}$ –C $_{12}$  and C $_6$ –C $_5$ –O $_{12}$ –C $_4$ –C $_3$ , that include the above-mentioned compressed C–O–C bond angles.

The intense C–O stretching vibration observed at 1102  $\text{cm}^{-1}$  in spectrum B (Figure 10) is obscured by intense broad bands corresponding to the Cl–O stretching mode (1072  $\text{cm}^{-1}$ ) for the hydrogen bonded perchlorate anion in compound **1** (Spectrum C, Figure 10) and by N–O stretching vibrations (1096  $\text{cm}^{-1}$ ) of the nitrito ligand (Spectrum A, Figure 10) in compound **2**. Additional features of the solid state IR spectrum of compound **1** include broad weak bands at 3554 and 3488  $\text{cm}^{-1}$  assigned to the O–H stretching modes of the symmetrically hydrogen bound water molecules, and a weak broadband at 1621  $\text{cm}^{-1}$  best interpreted as a vibration corresponding to a H $_2$ O bending mode.

## Conclusions

The dimercury(I) 18-crown-6 complex is sufficiently stable to permit isolation using traditional solution methods. The molecular structure of the complex, compound **1**, shows the mercurous Hg $_2^{2+}$  ion is irregularly centered within the macrocyclic cavity, defined by a  $D_{3d}$  conformation, known to encapsulate metals within an equatorial “girdle” of comparable mercury to oxygen interactions. Unusually long mercury to oxygen distances are observed for oxygen donor atoms of 18-crown-6 in compound **1**, proposed to arise from short H···H non-bonded interactions between adjacent macrocyclic rings across a Hg–Hg bond in the dimercury(I) cation. Steric interactions of this nature prevent closer approximation of ethereal oxygen donor atoms upon complexation, effectively lowering the basicity of the crown ether. Lowered ligand basicity disfavors complexation of the mercuric ion and consequently inhibits disproportionation, facilitating isolation of the dimercury(I) complex from solution.

Synthesis under hydrothermal conditions affords the mercuric nitrite complex of 18-crown-6, compound **2**. Lowered ligand basicity combined with the presence of elemental mercury, formed from the hydrothermal decomposition of mercuric nitrate, shift the disproportionation equilibrium in favor of the mercurous ion. The dimercury(I) complex, [(18-crown-6) $_2$ Hg $_2$ ](NO $_2$ ) $_2$ ], is proposed to initially form, followed by subsequent disproportionation products [(18-crown-6)Hg](NO $_2$ ) $_2$ ], the mercuric nitrite complex of 18-crown-6, and [(18-crown-6)Hg], a neutral mercury complex. The latter readily dissociates since the macrocyclic cavity of 18-crown-6 is unable to accommodate the size requirements of Hg $^0$ .

Selection of a suitable chelating agent, for incorporation into a small molecule mercury sensor or mercury polymer, should ideally be based upon specific mercury speciation characteristics of the selected chelating agent. This work shows that shifts in the mercury disproportionation equilibrium are important if crown ether derivatives are used as chelating agents in the development of mercury sensors.

**Acknowledgment.** The authors thank the University of North Carolina Wilmington, Wits Foundation, University of the Witwatersrand, South Africa, and the Anderson Capelli Trust Fund for their generous support.

**Supporting Information Available:** Cif files for complexes **1** and **2**. This material is available free of charge via the Internet at <http://pubs.acs.org>.